

# Can Millimeter Wave Cellular Systems provide High Reliability and Low Latency? An analysis of the impact of Mobile Blockers

Ish Kumar Jain, Rajeev Kumar, and Shivendra Panwar

Department of Electrical and Computer Engineering, Tandon School of Engineering, NYU, NY 11201, USA

**Abstract**—Millimeter Wave (mmWave) communication systems can provide high data rates, but the system performance may degrade significantly due to interruptions by mobile blockers such as humans or vehicles. A high frequency of interruptions and lengthy blockage durations will degrade the quality of the user's experience. A promising solution is to employ the macrodiversity of Base Stations (BSs), where the User Equipment (UE) can handover to other available BSs if the current serving BS gets blocked. However, an analytical model to evaluate the system performance of dynamic blockage events in this setting is unknown. In this paper, we develop a Line of Sight (LOS) dynamic blockage model and evaluate the probability, duration, and frequency of blockage events considering all the links in the range of the UE which are not blocked by buildings or the user's own body. For a dense urban area, we also analyze the impact of non-LOS (NLOS) links on blockage events. Our results indicate that the minimum density of BS required to satisfy the Quality of Service (QoS) requirements of Ultra Reliable Low Latency Communication (URLLC) applications is driven mainly by reliability and latency constraints, rather than coverage or capacity requirements.

**Index Terms**—Blockage, reliability, 5G, mmWave, stochastic geometry, URLLC, QoS, augmented reality, virtual reality, network planning.

## I. INTRODUCTION

Recent advancements in applications ranging from Machine-Type Communication (MTC) to mission-critical services (autonomous driving, eHealth, Augmented/Virtual Reality (AR/VR), and tactile Internet) are posing tremendous challenges regarding capacity, reliability, latency, and scalability. Autonomous driving, eHealth, and MTC may require low capacity, but impose a very tight constraint on the network for ultra-high service reliability (99.999%), ultra-low latency (1ms-10ms), and low Block Error Rates (BLER) ( $10^{-9} - 10^{-5}$ ) [1]–[3]. On the other hand, AR/VR applications require a significantly higher capacity (100 Mbps - few Gbps) and low latency (1ms-10ms), while being able to tolerate a relatively higher BLER [2]. The stringent requirements of these applications propel the rethinking of 5G cellular network design for Ultra Reliable Low Latency Communication (URLLC) applications. While many proposals to achieve low latency and high reliability have been proposed, such as edge caching, edge computing, network slicing [4], [5], a shorter Transmission Time Interval (TTI), frame structure [6], and flow queueing with dynamic sizing of the Radio Link Control (RLC) buffer at Data Link Layer [7], we focus our analysis on issues related to Radio Access Network (RAN) planning to achieve the stringent Quality of Service (QoS) requirements of URLLC applications.

Millimeter wave (mmWave) frequencies are being considered for the 5G RAN due to their abundant bandwidth as compared to traditional sub-6 GHz bands [8]. Thanks to the high bandwidth available at mmWave frequencies, the mmWave RAN can achieve data rates of the order of a few Gbps [9], suitable for the QoS requirements for AR/VR applications. However, mmWave communication systems are quite vulnerable to blockages due to higher penetration losses and reduced diffraction [10]. Even the human body can reduce the signal strength by 20 dB [11]. Thus, an unblocked Line of Sight (LOS) link is highly desirable for mmWave systems. When a LOS link is blocked, strong Non-Line of Sight (NLOS) links may also be helpful in achieving high reliability. However, NLOS links can also be blocked by mobile blockers. A mobile human blocker can block a link for approximately 500 ms [11]. The frequent blockages of mmWave links and a high blockage duration can be detrimental to URLLC applications.

One potential solution to blockages in the mmWave cellular network is employing a combination of macrodiversity of BSs and Coordinated Multipoint (CoMP) techniques. These techniques have shown a significant reduction in interference and improvement in reliability, coverage, and capacity in the current sub-6-GHz Long Term Evolution-Advance (LTE-A) deployments [12]. Furthermore, RANs are moving towards the cloud-RAN architecture that implements macrodiversity and CoMP techniques by pooling a large number of BSs in a single centralized Base Band Unit (BBU) [13], [14]. As a single centralized BBU handles multiple BSs, the handover and beam-steering time can be reduced significantly [15]. Furthermore, LTE BSs can help in achieving high reliability by serving as a backup in the case of a blockage of mmWave BSs. However, the LTE and 5G New Radio (NR) stacks must be coupled tightly for low handover delays. Note that the migration of services from 5G NR to LTE in case of blockages may cause up to 30 ms extra delay in the control plane [16]. The delay caused due to service migration from 5G NR to LTE can be reduced ( $\sim 10$  ms) by considering shorter TTI and processing delay at BSs. Thus, even though LTE and 5G NR interworking may increase the service reliability, it fails to satisfy latency requirements of URLLC applications if the two stacks are not tightly-coupled.

The impact of service interruptions due to blockage can also be alleviated by caching the downlink content at the BSs or the network edge for AR/VR applications [17]. However, caching the content more than about 10 ms may degrade the user experience and may cause nausea to the users particularly for AR applications [18]. For applications like MTC, autonomous

driving, eHealth, and the tactile Internet, the 5G network must achieve high reliability and low latency. Careful network planning can meet the requirements of URLLC applications. Therefore, it is important to study the blockage probability and blockage duration to satisfy the desired QoS requirements.

As shown in previous work by Bai, Vaze, and Heath [19], [20], mmWave networks may not provide a very high coverage due to static blockages (blockages such as buildings, trees, and other static structures). Thus, we envision the 5G cellular network as the overlap of LTE and 5G NR where the coverage holes of the 5G NR would be taken care of by LTE. In this architecture, both 5G and LTE will be collectively responsible for achieving QoS requirements of URLLC applications and the CRAN will be responsible for seamless migration of services from 5G NR to LTE (or vice-versa). Our primary concern is to quantify the QoS requirements of URLLC applications in the mmWave cellular network where blockages may cause a significant problem. To provide seamless connectivity for URLLC applications, we present an analysis considering key QoS parameters such as the probability of blockage events and the blockage duration. The major contributions of this paper are summarized as follows:

- 1) We provide a stochastic geometry based analytical model of the combined effect of static blockages (UE blocked by permanent structures such as buildings), dynamic blockage (UE blocked by mobile blockers) and self-blockage (UE blocked by the user's own body) to evaluate the impact on key QoS metrics.
- 2) For the open park scenario, we obtain closed-form expressions for probability and duration of simultaneous blockage of all BSs in the range of the UE. We also compare two models, one based on stochastic geometry and the other based on a hexagonal cell layout.
- 3) For urban scenarios, we consider the impact of static blockages and NLOS paths to obtain analytical expressions for blockage probability and duration.
- 4) We verify our dynamic blockage model through Monte-Carlo simulations by considering a random waypoint mobility model for mobile blockers.
- 5) Finally, we present a case study to find the minimum BS density that is required to satisfy the QoS requirements of URLLC applications for two scenarios: an open park-like scenario and an urban scenario. We also analyze the trade-off between BS height and density to satisfy the QoS requirements.

The rest of the paper is organized as follows. The related work is presented in Section II, and the system model is described in Section III. Section IV provides an analysis of blockage events and evaluates the key blockage metrics for LOS link. The analysis is extended to consider blockage of both LOS and NLOS links in Section V. Section VI considers the special case of a hexagonal cell layout. The validation of our theoretical results with simulations and various case studies are presented in Section VII. Finally, Section VIII concludes the paper.

## II. RELATED WORK

A mmWave link may have three kinds of blockages, namely, static, dynamic, and self-blockage. Static blockage due to buildings and permanent structures has been thoroughly studied by Bai, Vaze, and Heath in [19] and [20] using random shape theory and a stochastic geometry approach for urban microwave systems. The underlying static blockage model is incorporated into the cellular system coverage and rate analysis by Bai *et al.* [10]. Static blockage may cause permanent blockage of the LOS link. However, for an open area such as a public park, static blockages play a small role.

The second type of blockage is dynamic blockage due to mobile humans and vehicles (collectively called mobile blockers) which may cause frequent interruptions to the LOS link. Dynamic blockage has been given significant importance by 3GPP in TR 38.901 of Release 14 [21]. An analytical model in [22] considers a single access point, a stationary user, and blockers located randomly in an area. The model in [23] is developed for a specific scenario of a road intersection using a Manhattan Poisson point process model. MacCartney *et al.* [11] developed a Markov model for blockage events based on measurements on a single BS-UE link. Similarly, Raghavan *et al.* [24] fits the blockage measurements with various statistical models. However, a model based on experimental analysis is generally specific to the measurement scenario and may not generalize well to other scenarios. The authors in [25] considered a 3D blockage model and analyzed the blocker arrival probability for a single BS-UE pair. Studies of spatial correlation and temporal variation in blockage events for a single BS-UE link are presented in [26] and [27]. However, their analytical model is not easily scalable to multiple BSs.

Apart from static and dynamic blockage, self-blockage plays a significant role in mmWave performance. The authors of [28] studied human body blockage through simulation. A statistical self-blockage model is developed in [24] through experiments considering various modes (landscape or portrait) of hand-held devices. The impact of self-blockage on received signal strength is studied by Bai and Heath in [20] through a stochastic geometry model. They assume the self-blockage due to a user's body blocks the BSs in an area represented by a cone.

All the above blockage models consider the UE's association with a single BS. Macrodiversity of BSs is considered as a potential solution to alleviate the effect of blockage events in a cellular network. The authors of [29] and [30] proposed an architecture for macrodiversity with multiple BSs and showed improvements in network throughput. A blockage model with macrodiversity is developed in [31] for independent blocking and in [32] for correlated blocking. However, they consider only static blockage due to buildings.

The primary purpose of the blockage models in previous papers was to study the coverage and capacity analysis of the mmWave system. However, apart from the signal degradation, blockage frequency and duration also affects the performance of the mmWave system and are critically important for URLLC applications.

In our previous work [33], we presented the effect of

Table I: Summary of Notations

Notation	Description
$R$	LOS Radius.
$\tilde{R}$	NLOS Radius.
$\lambda_T$	BS Density.
$\lambda_B, \lambda_D$	Density of dynamic blockers, and static blockages resp.
$\alpha_i$	Arrival rate of dynamic blockers.
$\omega$	Self-blockage angle.
$m$	Number of BS in disc $B(o, R)$ .
$n$	Number of BS in coverage.
$k$	Number of NLOS links for a given BS.
$\kappa$	Parameter for number of NLOS Paths.
$r_i$	UE-BS distance.
$\mathcal{C}^d$	LOS coverage considering only self-blockage.
$\mathcal{C}^{LOS}$	LOS Coverage considering static and self-blockage.
$\mathcal{C}$	LOS and NLOS coverage considering static and self-blockage.
$B^s, B^d$	Indicator for static and dynamic blockage resp.
$B^{hex}$	Blockage indicator for hexagonal case.
$B^{LOS}$	LOS Blockage indicator considering static, dynamic, and self-blockage.
$B$	LOS and NLOS blockage indicator considering static, dynamic, and self-blockage.
$\zeta^d$	Blockage frequency considering only dynamic and self-blockage.
$T^d$	Blockage duration of LOS paths considering dynamic and self-blockage.
$T^{LOS}$	Blockage duration of LOS paths considering static, dynamic, and self-blockage without NLOS paths.
$T$	Blockage duration considering static, dynamic, and self-blockage with both LOS and NLOS paths.

dynamic blockage and self-blockage on the LOS link in an open park scenario. The results presented in [33] indicate that a high density of BS is required to satisfy the QoS requirements of URLLC applications. The study motivated us to consider a regular hexagonal cell layout in this paper. We showed that a well-planned cellular network such as the hexagonal layout could combat blockage events more efficiently than a random BS deployment in an open park scenario. Furthermore, in this paper, we also consider an urban setting, where static blockages may block the LOS paths between UE and BSs, and at the same time provide NLOS paths between UE and BSs. This paper extends our previous dynamic blockage analysis to include static blockages and derives the blockage probability and duration considering the blockage of LOS as well as NLOS paths.

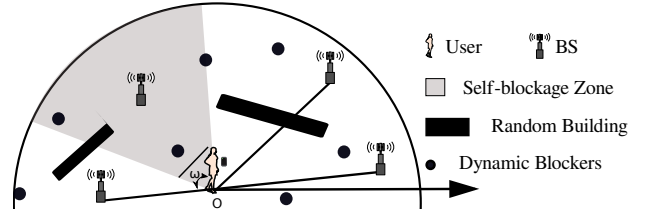
### III. SYSTEM MODEL

#### A. Assumptions

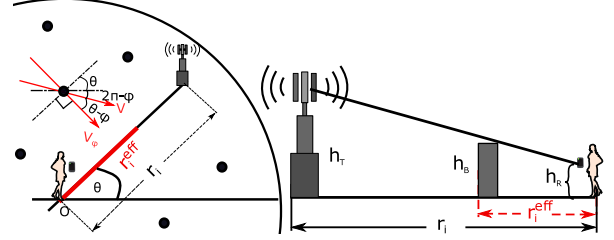
Various components of our system model and the associated assumptions are presented as follows:

- **BS Model:** The mmWave BS locations are modeled as a homogeneous Poisson Point Process (PPP) with density  $\lambda_T$  (a brief summary of notations is provided in Table I). Consider a disc  $B(o, R)$  of radius  $R$  and centered around the origin  $o$ , where a typical UE is located. We assume that each BS in  $B(o, R)$  is a potential serving BS for the UE. Thus, the number of BSs  $M$  in the disc  $B(o, R)$  of area  $\pi R^2$  follows a Poisson distribution with parameter  $\lambda_T \pi R^2$ , i.e.,

$$P_M(m) = \frac{[\lambda_T \pi R^2]^m}{m!} e^{-\lambda_T \pi R^2}. \quad (1)$$



(a) Types of blockages



(b) Dynamic blockage model

Figure 1: System Model: (a) Service quality to the UE can be degraded by static blockage, self-blockage, and dynamic blockages. A typical UE is located at the center and BSs and blockers are located uniformly in a disc around the UE. (b) Dynamic blockers are moving with velocity  $V$  at a random angle  $\varphi$  from the x-axis. A blocker within  $r_i^{eff}$  distance away from the UE can cause interruptions to the  $i$ th BS-UE link.

Given the number of BSs  $m$  in the disc  $B(o, R)$ , we have a uniform probability distribution for BS locations. The BSs distances  $R_i, \forall i = 1, \dots, m$ , from the UE are independent and identically distributed (i.i.d.) with distribution

$$f_{R_i|M}(r|m) = \frac{2r}{R^2}; \quad 0 < r \leq R, \forall i = 1, \dots, m. \quad (2)$$

- **Static Blockage Model:** The static blockage due to buildings and permanent structures is thoroughly studied by Bai and Heath [20]. They modeled the static blockages such as buildings using random shape theory. The buildings are considered to be of length  $\ell$ , and width  $w$ . The probability<sup>1</sup>  $P(B_i^s|m, r_i)$  that the  $i$ th BS-UE link is not blocked by any building is calculated in [20] as

$$P(B_i^s|m, r_i) = 1 - e^{-(\beta r_i + \beta_0)}; \quad \forall i = 1, \dots, m, \quad (3)$$

where  $\beta = \frac{2}{\pi} \lambda_D (\mathbb{E}[\ell] + \mathbb{E}[w])$  and  $\beta_0 = \lambda_D \mathbb{E}[\ell] \mathbb{E}[w]$ ; where  $\lambda_D$  is density of static blockage represented in terms of static blockages per km<sup>2</sup> (sbl/km<sup>2</sup>), and  $\mathbb{E}[\ell]$  and  $\mathbb{E}[w]$  are the expected length and width of buildings respectively. The effect of the height of buildings on static blockage probability is analyzed in [20]. For simplicity, we assume the static blockages are higher than the BS.

- **Self-blockage Model:** The user blocks a fraction of BSs due to his/her own body. The self-blockage zone is defined as a sector of the disc  $B(o, R)$  making an angle  $\omega$  towards the user's body as shown in Figure 1(a). The orientation of the user's body is uniform in  $[0, 2\pi]$ . We

<sup>1</sup>Note that the notation  $P(B_i^s|m, r_i)$  is a compressed version of  $P_{B_i^s|M, R_i}(B_i^s|m, r_i)$ , which we use for convenience. Similar notations used elsewhere in this paper should be clear based on the context.

consider a BS is blocked by the self-blockage if it lies in the self-blockage zone. Therefore, the probability that a randomly chosen BS is not blocked by self-blockage is

$$p = 1 - \frac{\omega}{2\pi}. \quad (4)$$

- **Dynamic Blockage Model:** Dynamic blockers are distributed according to a homogeneous PPP with density  $\lambda_B$  represented in terms of blockers per  $\text{m}^2$  ( $\text{bl}/\text{m}^2$ ). The blockers are moving in the disc  $B(o, R)$  with velocity  $V$  in a random direction. Further, the arrival process of the blockers crossing the  $i$ th BS-UE link is Poisson with intensity  $\alpha_i$ . We derive an expression for  $\alpha_i$  in the next subsection. The blockage duration is independent of the blocker arrival process and is exponentially distributed with parameter  $\mu$ . In the rest of the paper, the term *blocker* implies dynamic blockers, unless otherwise stated.
- **NLOS Model:** NLOS links can fill the coverage holes in the mmWave cellular system and can even enhance the reliability. However, the signal degradation, due to reflections from reflectors such as buildings, may limit the number of strong NLOS paths. Since the NLOS link length is always longer than the corresponding LOS link length, we only consider those NLOS paths which correspond to BSs within  $\tilde{R} \leq R$  distance from the origin. The corresponding disc  $B(o, \tilde{R})$  is shown in Figure 2. The number of NLOS links  $K$  for a given BS-UE pair was obtained by Akdeniz *et al.* [9] through measurements in an urban area as

$$K \sim \max\{\text{Poisson}(\kappa), 1\}, \quad (5)$$

where  $\kappa$  is obtained empirically. The distribution  $P_K(k)$  follows:

$$P_K(k) = \begin{cases} 0 & \text{if } k = 0, \\ e^{-\kappa} + e^{-\kappa}\kappa & \text{if } k = 1, \\ \frac{e^{-\kappa}\kappa^k}{k!} & \text{if } k > 1. \end{cases} \quad (6)$$

We consider virtual locations of NLOS BSs as images of LOS BS via reflectors. For a given BS at a distance  $r_i$  from origin, the corresponding virtual BSs would be at a distance longer than  $r_i$ . To obtain a lower bound on blockage probability, we consider the best case scenario when the NLOS BSs are located exactly at a distance  $r_i$  from origin. For simplicity, we assume the virtual BSs are distributed uniformly in a ring of radius  $r_i$ , which is same as the actual BS-UE link length.

- **Connectivity Model:** We say the UE is blocked when all of the potential serving BSs, actual and virtual, in the disc  $B(o, R)$  are blocked simultaneously.

### B. Dynamic Blockage Model for a Single BS-UE Link

For a sound understanding of the system model, consider a single BS-UE LOS link in Figure 1(b). The 2D distance between the  $i$ th BS and the UE is  $r_i$ , and the LOS link makes an angle  $\theta$  from the positive x-axis in the azimuth plane. Further, the blockers in the region move with constant velocity  $V$  at an angle  $\varphi$  with the positive x-axis, where

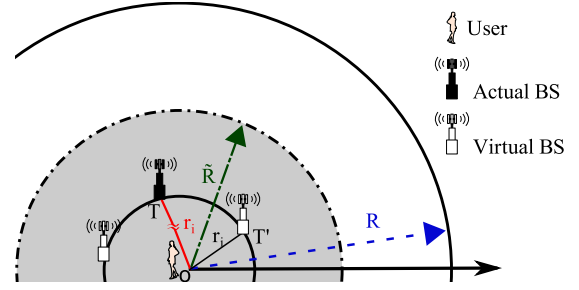


Figure 2: NLOS model: The shaded region (a disc  $B(o, \tilde{R})$  of radius  $\tilde{R}$ ) represents the NLOS zone such that an actual BS in this region may provide strong NLOS signals. For a given BS at a distance  $r_i$  from the origin, the corresponding virtual BSs are also shown.

$\varphi \sim \text{Unif}([0, 2\pi])$ . Note that only a fraction of blockers crossing the BS-UE link will be blocking the LOS path, as shown in Figure 1(b). The effective link length  $r_i^{eff}$  that is affected by the movement dynamic blockers is given by,

$$r_i^{eff} = \frac{(h_B - h_R)}{(h_T - h_R)} r_i, \quad (7)$$

where  $h_B$ ,  $h_R$ , and  $h_T$  are the heights of blocker, UE (receiver), and BS (transmitter) respectively. The blocker arrival rate  $\alpha_i$  (also called the blockage rate) is evaluated in Lemma 1.

**Lemma 1.** *The blockage rate  $\alpha_i$  of the  $i$ th BS-UE link is*

$$\alpha_i = C r_i, \quad (8)$$

where  $C$  is proportional to blocker density  $\lambda_B$  as,

$$C = \frac{2}{\pi} \lambda_B V \frac{(h_B - h_R)}{(h_T - h_R)}. \quad (9)$$

*Proof.* Consider a blocker moving at an angle  $(\theta - \varphi)$  relative to the BS-UE link (See Figure 1(b)). The component of the blocker's velocity perpendicular to the BS-UE link is  $V_\varphi = V \sin(\theta - \varphi)$ , where  $V_\varphi$  is positive when  $(\theta - \pi) < \varphi < \theta$ . Next, we consider a rectangle of length  $r_i^{eff}$  and width  $V_\varphi \Delta t$ . The blockers in this area will block the LOS link over the interval of time  $\Delta t$ . Note there is an equivalent area on the other side of the link. Therefore, the frequency of blockage is  $2\lambda_B r_i^{eff} V_\varphi \Delta t = 2\lambda_B r_i^{eff} V \sin(\theta - \varphi) \Delta t$ . Thus, the frequency of blockage per unit time is  $2\lambda_B r_i^{eff} V \sin(\theta - \varphi)$ . Taking an average over the uniform distribution of  $\varphi$  (uniform over  $[0, 2\pi]$ ), we get the blockage rate  $\alpha_i$  as follows:

$$\begin{aligned} \alpha_i &= 2\lambda_B r_i^{eff} V \int_{\varphi=\theta-\pi}^{\theta} \sin(\theta - \varphi) \frac{1}{2\pi} d\varphi \\ &= \frac{2}{\pi} \lambda_B r_i^{eff} V = \frac{2}{\pi} \lambda_B V \frac{(h_B - h_R)}{(h_T - h_R)} r_i. \end{aligned} \quad (10)$$

This concludes the proof.  $\blacksquare$

Following [27], we model the blocker arrival process as Poisson with parameter  $\alpha_i$  blockers/sec ( $\text{bl}/\text{s}$ ). Note that there can be more than one blocker simultaneously blocking the LOS link. The overall blocking process has been modeled in [27] as an alternating renewal process with alternate periods of blocked/unblocked intervals, where the distribution of the blocked interval is obtained as the busy period distribution of a general  $M/GI/\infty$  system. For mathematical simplicity,

we assume the blockage duration of a single blocker is exponentially distributed with parameter  $\mu$ , thus, forming the blocker arrival process as an  $M/M/\infty$  queuing system. We further approximate the overall blocking process as an alternating renewal process with exponentially distributed periods of blocked and unblocked intervals with parameters  $\alpha_i$  and  $\mu$  respectively. This approximation works for a wide range of blocker densities, as is verified in Section VII.

The blocking event of a BS-UE link follows an on-off process with  $\alpha_i$  and  $\mu$  as blocking and unblocking rates, respectively. The probability of blockage  $P(B_i^d|m, r_i)$  of the  $i$ th BS-UE link due to dynamic blockers follows:

$$P(B_i^d|m, r_i) = \frac{\alpha_i}{\alpha_i + \mu} = \frac{\frac{C}{\mu} r_i}{1 + \frac{C}{\mu} r_i}, \quad (11)$$

where  $C$  is proportional to the blocker density  $\lambda_D$  as defined in (9). For readers interested in obtaining state probabilities other than blockage, a Markov chain analysis for dynamic blockages is presented in Appendix G.

In the next section, we consider a generalized LOS blockage model considering all three kind of blockages. We assume the UE keeps track of all available BSs using beam-tracking and handover protocols. Since the handover process is assumed to be of short duration as compared to the average duration of the blockage event, we assume that the UE can instantaneously connect to any unblocked BS when the current serving BS gets blocked. Therefore, we consider the total blockage event occurs only when all the potential serving BSs are blocked.

#### IV. GENERALIZED LOS BLOCKAGE MODEL

##### A. Coverage Probability

We say that the UE is in coverage if there is at least one BS not blocked by either static blockage or by self-blockage.

**Lemma 2.** *The distribution of the number of BSs ( $N$ ) which are not blocked by static or self-blockage follows a Poisson distribution with parameter  $pq\lambda_T\pi R^2$ , i.e.,*

$$P_N(n) = \frac{[pq\lambda_T\pi R^2]^n}{n!} e^{-pq\lambda_T\pi R^2}, \quad (12)$$

where,

$$p = 1 - \omega/2\pi, \text{ and, } q = \frac{2e^{-\beta_0}}{\beta^2 R^2} \left[ 1 - (1 + \beta R)e^{-(\beta R)} \right] \quad (13)$$

*Proof.* See Appendix A. ■

**Corollary 1.** *Let  $\mathcal{C}^{LOS}$  denote the LOS coverage event that represents that the UE has at least one serving BS in the disc  $B(o, R)$  and is not blocked by static or self-blockage. The probability of this LOS coverage event  $\mathcal{C}^{LOS}$  is calculated as*

$$P(\mathcal{C}^{LOS}) = 1 - P_N(0) = 1 - e^{-pq\lambda_T\pi R^2}. \quad (14)$$

##### B. LOS Blockage Probability

Our objective is to develop a blockage model for the mmWave cellular system where the UE can connect to any of the potential serving BSs. In this setting, the blockage occurs when all the BS-UE links are blocked simultaneously.

We define an indicator random variable  $B^{LOS}$  that indicates the LOS blockage of all available BSs in the range of the UE. We obtain the blockage probability by utilizing the independence of static, dynamic, and self-blockage events. The LOS blockage probability  $P(B_i^{LOS}|m, r_i)$  of the  $i$ th BS-UE link is conditioned on the number of BSs  $m$  in the disc  $B(o, R)$  and the BS-UE distance  $r_i$ , and is given by:

$$\begin{aligned} P(B_i^{LOS}|m, r_i) &= 1 - p(1 - P(B_i^s|m, r_i))(1 - P(B_i^d|m, r_i)) \\ &= 1 - pe^{-(\beta r_i + \beta_0)} \frac{1}{1 + \frac{C}{\mu} r_i}, \end{aligned} \quad (15)$$

where we use the expressions for static and dynamic blockage probability from (3) and (11) respectively. The blockage events of multiple BSs may be correlated based on the location of dynamic blockers. For instance, a blocker closer to the user may simultaneously block multiple BSs as compared to a blocker farther away from the the user. However, in this paper, we assume independent blockage of all the BS-UE links and leave the correlation analysis for our future work. Denoting the set of distances  $\{r_1, r_2, \dots, r_m\}$  by a compressed form  $\{r_i\}$ , we evaluate the probability of simultaneous blockage of all the LOS BS-UE links, i.e.,  $P(B^{LOS}|m, \{r_i\})$ , as follows:

$$\begin{aligned} P(B^{LOS}|m, \{r_i\}) &= \prod_{i=1}^m (P(B_i^{LOS}|m, r_i)) \\ &= \prod_{i=1}^m \left( 1 - pe^{-(\beta r_i + \beta_0)} \frac{1}{1 + \frac{C}{\mu} r_i} \right). \end{aligned} \quad (16)$$

To obtain the unconditional or marginal LOS blockage probability  $P(B^{LOS})$ , we first evaluate the conditional LOS blockage probability  $P(B^{LOS}|m)$  by taking the average of  $P(B^{LOS}|m, \{r_i\})$  over the distribution of distances  $\{r_i\}$  and then find  $P(B^{LOS})$  by taking the average of  $P(B^{LOS}|m)$  over the distribution of  $m$  as follows:

$$P(B^{LOS}|m) = \iint_{r_i} P(B^{LOS}|m, \{r_i\}) f(\{r_i\}|m) dr_1 \cdots dr_m \quad (17)$$

$$P(B^{LOS}) = \sum_{m=0}^{\infty} P(B^{LOS}|m) P_M(m). \quad (18)$$

**Theorem 1.** *The marginal LOS blockage probability and the conditional LOS blockage probability given LOS coverage (14) is given by:*

$$P(B^{LOS}) = e^{-ap\lambda_T\pi R^2}, \quad (19)$$

$$P(B^{LOS}|\mathcal{C}^{LOS}) = \frac{e^{-ap\lambda_T\pi R^2} - e^{-pq\lambda_T\pi R^2}}{1 - e^{-pq\lambda_T\pi R^2}}, \quad (20)$$

where,

$$a = \int_r \frac{e^{-(\beta r + \beta_0)}}{1 + \frac{C}{\mu} r} \frac{2r}{R^2} dr \quad (21)$$

can be computed by numerical integration. Note that  $C$  is proportional to blocker density  $\lambda_B$  as shown in (9). Also,  $p$

and  $q$  are defined in (13) and are functions of the self-blockage angle  $\omega$ , and static blockage density  $\lambda_D$ , respectively.

*Proof.* See Appendix B. ■

We also consider an open park scenario, with no static blockages, and obtain a closed-form expression for the blockage probability considering only dynamic and self-blockage.

**Corollary 2.** *The coverage probability  $P(\mathcal{C}^d)$  for an open park scenario is given by*

$$P(\mathcal{C}^d) = e^{-p\lambda_T\pi R^2}. \quad (22)$$

The LOS dynamic blockage probability  $P(B^d|\mathcal{C}^d)$ , conditioned on coverage  $\mathcal{C}^d$ , is given by

$$P(B^d|\mathcal{C}^d) = \frac{e^{-a'p\lambda_T\pi R^2} - e^{-p\lambda_T\pi R^2}}{1 - e^{-p\lambda_T\pi R^2}}, \quad (23)$$

where,

$$a' = \frac{2\mu}{RC} - \frac{2\mu^2}{R^2C^2} \log\left(1 + \frac{RC}{\mu}\right). \quad (24)$$

The proof is given in Appendix B.

The closed-form expression of blockage probability for the open park scenario gives insights while facilitating a quick analysis for network planning. For instance, we can approximate  $a$  by taking a series expansion of  $\log(1 + RC/\mu)$ , i.e.,

$$\begin{aligned} a' &= \frac{2\mu}{RC} - \frac{2\mu^2}{R^2C^2} \left( \frac{RC}{\mu} - \frac{R^2C^2}{2\mu^2} + \frac{R^3C^3}{3\mu^3} + \dots \right), \\ &\approx 1 - \frac{2RC}{3\mu}, \quad \text{when } \frac{RC}{\mu} \ll 1. \end{aligned} \quad (25)$$

Note that for the blocker density as high as 0.1 bl/m<sup>2</sup>, and for other parameters in Table III, we have  $RC/\mu = 0.35$ , which shows that the approximation (25) holds for a wide range of blocker densities. For large BS density  $\lambda_T$ , the coverage probability  $P(\mathcal{C}^d)$  is approximately 1 and  $P(B^d|\mathcal{C}^d) \approx P(B^d)$ . In order to have the blockage probability  $P(B^d)$  less than a threshold  $\bar{P}$ , i.e.,

$$P(B^d) = e^{-a'p\lambda_T\pi R^2} \leq \bar{P}, \quad (26)$$

the required BS density follows

$$\lambda_T \geq \frac{-\log(\bar{P})}{a'p\pi R^2} \approx \frac{-\log(\bar{P})(1 + \frac{2RC}{3\mu})}{p\pi R^2}, \quad (27)$$

where  $C$  is proportional to the blocker density  $\lambda_B$  in (9). The result (27) shows that the BS density approximately scales linearly with the blocker density (along with a constant factor).

### C. Expected Blockage Duration

Recall that the duration of the blockage of a single BS-UE link is an exponential random variable with mean  $1/\mu$ . Since the blockage of individual BS-UE links are independent, the duration  $T^{LOS}$  of the LOS blockage of all  $n$  BSs follows an exponential distribution with mean  $1/n\mu$ . We can therefore write the expected LOS blockage duration as

$$\mathbb{E}[T^{LOS}|n] = \frac{1}{n\mu}. \quad (28)$$

**Theorem 2.** *The expected blockage duration of simultaneous blockage of all the BSs in  $B(o, R)$ , conditioned on the coverage event  $\mathcal{C}^{LOS}$  in (14), is obtained as*

$$\mathbb{E}[T^{LOS}|\mathcal{C}^{LOS}] = \frac{e^{-pq\lambda_T\pi R^2}}{\mu(1 - e^{-pq\lambda_T\pi R^2})} Ei[pq\lambda_T\pi R^2], \quad (29)$$

where,  $Ei[pq\lambda_T\pi R^2] = \sum_{n=1}^{\infty} \frac{[pq\lambda_T\pi R^2]^n}{nn!}$ . Also,  $p$  and  $q$  are defined in (13).

*Proof.* See Appendix C. ■

**Lemma 3.**  *$Ei[pq\lambda_T\pi R^2]$  converges.*

*Proof.* We can use Cauchy ratio test to show that the series  $\sum_{n=1}^{\infty} \frac{[pq\lambda_T\pi R^2]^n}{nn!}$  is convergent. Consider  $L = \lim_{n \rightarrow \infty} \frac{[pq\lambda_T\pi R^2]^{n+1}/((n+1)(n+1)!)}{[pq\lambda_T\pi R^2]^n/(nn!)} = \lim_{n \rightarrow \infty} \frac{[pq\lambda_T\pi R^2]^{n+1}}{(n+1)^2} = 0$ . Hence, the series converges. ■

An approximation of blockage duration (29) can be obtained for a high BS density ( $\lambda_T$ ) as follows:

$$\begin{aligned} \mathbb{E}[T^{LOS}|\mathcal{C}^{LOS}] &\approx \frac{1}{\mu(1 - e^{-pq\lambda_T\pi R^2})} \left( \frac{1}{pq\lambda_T\pi R^2} + \frac{1}{(pq\lambda_T\pi R^2)^2} \right) \\ &\approx \frac{1}{\mu pq\lambda_T\pi R^2 (1 - e^{-pq\lambda_T\pi R^2})}. \end{aligned} \quad (30)$$

This approximation is justified in Appendix D.

**Corollary 3.** *The expected blockage duration for open park scenario is given by*

$$\mathbb{E}[T^d|\mathcal{C}^d] = \frac{e^{-p\lambda_T\pi R^2}}{\mu(1 - e^{-p\lambda_T\pi R^2})} Ei[p\lambda_T\pi R^2], \quad (31)$$

which can be obtained from (29), by setting  $q = 1$  (corresponding to  $\beta = 0$  and  $\beta_0 = 0$ ).

### D. Expected Blockage Frequency

For the open park scenario, we define dynamic blockage frequency  $\zeta^d$  as the rate of blockage of all the BSs in the range of UE, i.e.,

$$\zeta^d = n\mu P(B^d|n, \{r_i\}), \quad (32)$$

where  $P(B^d|n, \{r_i\})$  represents the dynamic blockage probability given  $n$  and  $\{r_i\}$ ; where  $n$  is the number of BS in the disc  $B(o, R)$  not blocked by the user's body and  $\{r_i\}$  is the set of UE-BS distances  $r_i$ , for  $i = 1, \dots, n$ . We do not consider the effect of static blockages for the open park scenario. A closed-form expression for expected blockage frequency is obtained in Theorem 3.

**Theorem 3.** *The expected blockage frequency given coverage  $\mathcal{C}^d$  (22) for the open park scenario is obtained as:*

$$\mathbb{E}[\zeta^d|\mathcal{C}^d] = \frac{\mu(1 - a')p\lambda_T\pi R^2 e^{-a'p\lambda_T\pi R^2}}{1 - e^{-p\lambda_T\pi R^2}}. \quad (33)$$

where  $p$  and  $a'$  are defined in (4) and (24) respectively.

*Proof.* See Appendix E. ■

## V. EFFECT OF NLOS LINKS ON BLOCKAGE

In the previous section, we analyzed the LOS blockage probability and duration of blockage events due to mobile blockers. Apart from the LOS signal, the NLOS paths through reflections by buildings, trees and other permanent structures (collectively called reflectors) also play a major role in the mmWave cellular systems. Akdeniz *et al.* [9] have shown through measurements that there would be at least one NLOS path available for each BS-UE link. We therefore extend our blockage model to the NLOS links for a complete blockage analysis of mmWave cellular system. We first present a NLOS link model and evaluate the coverage probability by incorporating the NLOS links. Then we will evaluate a lower bound on the blockage probability given coverage by considering both LOS and NLOS links.

### A. Coverage Probability incorporating NLOS links

When we consider both LOS and NLOS links as potential links for connectivity, the coverage is defined as the availability of at least one unblocked LOS or NLOS link (unblocked by static or self-blockage). Considering the experimental results by Akdeniz *et al.* [9], there is always at least one NLOS signal for a given BS location, and we assume the NLOS signal is sufficiently strong when the BS is in a disc  $B(o, \tilde{R})$  around the UE (See Figure 2). Therefore, we say that an NLOS link is not available when  $r_i > \tilde{R}$ , which we indicate by  $I_{(r_i > \tilde{R})}$ . Assuming the availability of LOS and NLOS links to be independent, we have

$$P(\mathcal{C}|m, \{r_i\}) = 1 - \prod_{i=1}^m \left(1 - pe^{-(\beta r_i + \beta_0)}\right) I_{(r_i > \tilde{R})}. \quad (34)$$

**Lemma 4.** *The coverage probability considering LOS and NLOS links is defined by*

$$P(\mathcal{C}) = 1 - e^{-\tilde{q}\lambda_T\pi R^2}, \quad (35)$$

where,

$$\tilde{q} = \frac{\tilde{R}^2}{R^2} - \frac{2pe^{-\beta_0}}{\beta^2\tilde{R}^2} \left( (1 + \beta R)e^{-\beta R} - (1 + \beta\tilde{R})e^{-\beta\tilde{R}} \right). \quad (36)$$

*Proof.* The proof is provided in Appendix F ■

### B. Incorporating NLOS links in Blockage Probability

The NLOS links can potentially help in achieving high coverage and reducing the blockage probability. In general, for a given BS at a distance  $r_i$  from the origin, the corresponding  $k$  virtual BSs are located at a distance larger than  $r_i$ . The corresponding NLOS link length can be obtained by tracing the path from the BS to a reflection point (point where the NLOS signal got reflected), and then from the reflection point to the UE. However, in order to avoid the underlying complexity, we present a lower bound on blockages for the NLOS case by considering all the  $k$  virtual BSs located at distance  $r_i$  from the origin, and uniformly over an angular range of  $[0, 2\pi]$ . By thus minimizing the length of NLOS paths and making their angular range independent of the

BS, we will minimize the incidence of blockage. For such a scenario, the NLOS blockage probability  $P(B_i^{NLOS}|m, r_i, k)$ , corresponding to the  $i$ th BS, considering blockage by dynamic blockers, is given by:

$$\begin{aligned} P(B_i^{NLOS}|m, r_i, k) &= \prod_{j=1}^k \left( \frac{\frac{C}{\mu} r_i}{1 + \frac{C}{\mu} r_i} I_{(r_i \leq \tilde{R})} + 1 - I_{(r_i \leq \tilde{R})} \right) \\ &= \prod_{j=1}^k \left( 1 - \frac{1}{1 + \frac{C}{\mu} r_i} I_{(r_i \leq \tilde{R})} \right) \\ &= \left( 1 - \frac{1}{1 + \frac{C}{\mu} r_i} I_{(r_i \leq \tilde{R})} \right)^k \\ &= (1 - \tilde{b}(r_i))^k, \end{aligned} \quad (37)$$

where we assume the independent blocking of all the NLOS links and define  $\tilde{b}(r_i) = \frac{1}{1 + \frac{C}{\mu} r_i} I_{(r_i \leq \tilde{R})}$ . Next, we integrate the blockage probability in (37) w.r.t. the distribution of  $k$  given in (6) as follows:

$$\begin{aligned} P(B_i^{NLOS}|m, r_i) &= \sum_{k=1}^{\infty} P(B_i^{NLOS}|m, r_i, k) P_K(k) \\ &= \sum_{k=1}^{\infty} (1 - \tilde{b}(r_i))^k P_K(k). \end{aligned} \quad (38)$$

We further solve (38) and write the final expression as follow:

$$P(B_i^{NLOS}|m, r_i) = e^{-\tilde{b}(r_i)\kappa} - \tilde{b}(r_i)e^{-\kappa}. \quad (39)$$

The blockage probability  $P(B)$  follows by assuming independent blocking of LOS and NLOS links and by averaging over the distributions  $P_M(m)$  and  $f(\{r_i\}|m)$ , given in (1) and (2), respectively, as follow:

$$\begin{aligned} P(B) &= \sum_{m=0}^{\infty} \int \int_{r_i} \prod_{i=1}^m P(B_i^{LOS}|m, r_i) P(B_i^{NLOS}|m, r_i) \\ &\quad \times f(\{r_i\}|m) d\{r_i\} P_M(m). \end{aligned} \quad (40)$$

The final expression of the blockage probability  $P(B)$  is given in Theorem 4.

**Theorem 4.** *The blockage probability  $P(B)$  considering both LOS and NLOS links is given by,*

$$P(B) = e^{-\tilde{a}\lambda_T\pi R^2}, \quad (41)$$

where  $\tilde{a}$  is obtained as,

$$\tilde{a} = 1 - \int_r \left( 1 - \frac{pe^{-(\beta r + \beta_0)}}{1 + \frac{C}{\mu} r} \right) \left( e^{-\tilde{b}(r)\kappa} - \tilde{b}(r)e^{-\kappa} \right) \frac{2r}{R^2} dr. \quad (42)$$

The conditional probability given coverage  $\mathcal{C}$  (35) is given by

$$P(B|\mathcal{C}) = \frac{e^{-\tilde{a}\lambda_T\pi R^2} - e^{-\tilde{q}\lambda_T\pi R^2}}{1 - e^{-\tilde{q}\lambda_T\pi R^2}}, \quad (43)$$

where  $\tilde{q}$  and  $\tilde{a}$  are given in (36) and (42) respectively.

The proof follows by putting the expressions (15) and (39) in (40) and following the steps similar to the proof of Theorem 1 in Appendix B

### C. Approximate Expected Duration of Blockage considering NLOS links

Similar to the LOS case, we can evaluate the the expected duration of blockage events assuming independent blocking of LOS and NLOS links. We define the number of BS in the disc  $B(o, \tilde{R})$  as  $\tilde{n}$ , which follows  $\tilde{n} \sim \text{Poisson}(\lambda_T \pi \tilde{R}^2)$ . Given a BS in  $B(o, \tilde{R})$ , there are  $k$  virtual BSs corresponding to that actual BS. Therefore, the total number of NLOS links are  $\tilde{n}k$ . We know from Section IV that  $n$  LOS paths cover the UE. Therefore, the total number of LOS and NLOS paths is  $n + \tilde{n}k$ . The expected blockage duration is defined as

$$\mathbb{E}[T|C] = \frac{1}{1 - e^{-\tilde{q}\lambda_T\pi R^2}} \mathbb{E}\left[\frac{1}{\mu(n + \tilde{n}k)}\right], \quad (44)$$

where the expectation is taken over the distribution of  $n$ ,  $\tilde{n}$ , and  $k$ . We can approximate the blockage duration in (44) using first order approximation as follows:

$$\begin{aligned} \mathbb{E}[T|C] &\approx \frac{1}{1 - e^{-\tilde{q}\lambda_T\pi R^2}} \frac{1}{\mathbb{E}[\mu(n + \tilde{n}k)]} \\ &= \frac{1}{1 - e^{-\tilde{q}\lambda_T\pi R^2}} \frac{1}{\mu(\mathbb{E}[n] + \mathbb{E}[\tilde{n}]\mathbb{E}[k])} \\ &= \frac{1}{1 - e^{-\tilde{q}\lambda_T\pi R^2}} \frac{1}{\mu(pq\lambda_T\pi R^2 + \kappa\lambda_T\pi\tilde{R}^2)}, \end{aligned} \quad (45)$$

where (45) is a good approximation of blockage duration for high BS densities as discussed in Appendix D.

## VI. HEXAGONAL CELL LAYOUT

In Section IV, we analyzed the random deployment of BS in an area. We observed that a high density of BS is required to meet the QoS requirements (See Section VII). These results motivated us to look at a planned network such as a grid-based hexagonal cell layout for the open park scenario. For such a planned network, we analyze the probability of blockage events due to random mobile blockers. We consider a hexagonal cell layout shown in Figure 3. A typical BS is located at the origin, and the UE is located within that cell at a distance  $\delta$  from the origin and angle  $\rho$  from the x-axis. The user location is uniform in the central hexagonal cell. The other cells follow the hexagonal grid around the central cell. The distances  $d_i$  and angles  $\psi_i$  of BSs at different cells are given in Table II and shown in Figure 3. The distance  $r_i$  of the UE from the  $i$ th BS is given by:

$$r_i^2 = d_i^2 + \delta^2 - 2d_i\delta \cos(\psi_i - \rho), \quad (46)$$

which is a function of the UE's random location  $\{\delta, \rho\}$ .

For self-blockage, we consider a circle around UE of radius  $R$  and define a sector of this circle with an angle  $\omega$  as the self-blockage zone. We consider the worst case of self-blockage by choosing a location and orientation of the user which accounts for the blockage of the maximum number of BSs. For instance, for  $\omega = 60^\circ$ , there can be up to 10 BSs blocked by self-blockage out of total 37 BSs (See Table II and Figure 3).

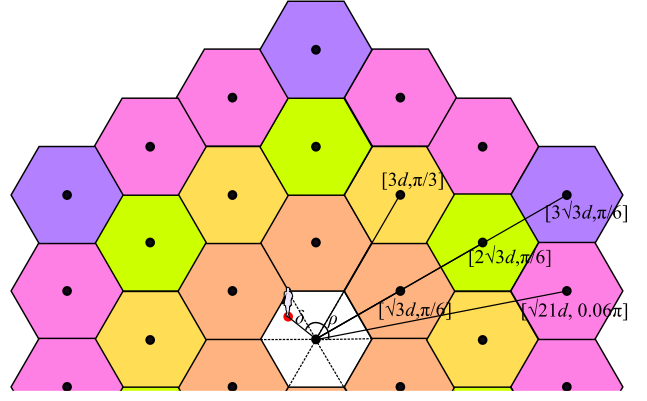


Figure 3: Hexagonal cellular layout.

Table II: Hexagonal cell distances and angular distributions.

Level	distance $d_i$	angle $\psi_i$	Num BS
0	0	reference	1
1	$\sqrt{3}d$	$[\pm\pi/6, \pm\pi/2, \pm5\pi/6]$	6
2	$3d$	$[0, \pm\pi/3, \pm2\pi/3, \pi]$	6
3	$2\sqrt{3}d$	$[\pm\pi/6, \pm\pi/2, \pm5\pi/6]$	6
4	$\sqrt{21}d$	$[\pm0.06\pi, \pm\pi/3 \pm 0.06\pi, \pm2\pi/3 \pm 0.06\pi, \pm(\pi - 0.06\pi)]$	12
5	$3\sqrt{3}d$	$[\pm\pi/6, \pm\pi/2, \pm5\pi/6]$	6

Considering this worst-case scenario, we get an upper bound on the blockage probability when we consider self-blockage.

The expression for dynamic blockage probability for the hexagonal case can be obtained by using the expression in (11) and assuming the independent blocking of all the links as follows:

$$P(B^{hex}|\delta, \rho) = \prod_{i=1}^{m'} \left(1 - \frac{1}{1 + \frac{c}{\mu} r_i}\right), \quad (47)$$

where  $m'$  is the number of BSs which are not blocked by self-blockage, and  $r_i$  for  $i = 1, \dots, m'$  is a function of  $(\delta, \rho)$ , as given in (46). We perform a numerical integration over the distribution of the UE's location  $\{\delta, \rho\}$ , assuming the UE is uniformly located in the central hexagon.

## VII. NUMERICAL EVALUATION

In this section, we evaluate our analysis for two different scenarios as follows:

- *Open park scenario:* In an open park scenario, due to lack of buildings and permanent structures, we assume that the UE does not suffer static blockages. We also assume that due to the lack of reflecting surfaces, we may not have strong NLOS paths available. Thus, we only considered dynamic and self-blockage of LOS links in this scenario.
- *Urban scenario:* In the case of an urban scenario, the signal to the UE may suffer static blockages due to buildings. At the same time, it may also have many NLOS paths available due to reflections by buildings and other structures. We evaluate our blockage analysis in the urban area with static blockages, LOS and NLOS paths along with dynamic and self-blockage.

The typical parameters used for simulation and numerical evaluation are presented in the Table III.

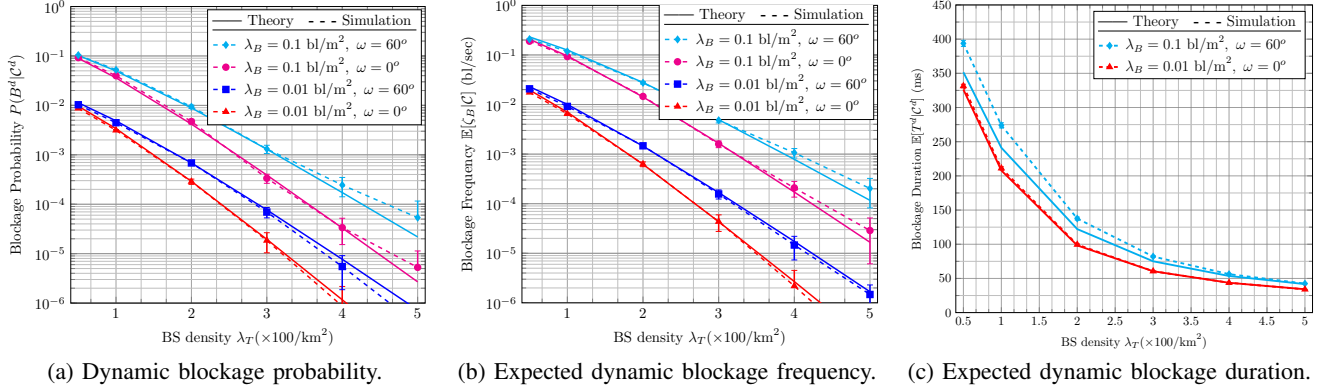


Figure 4: Conditional dynamic blockage statistics given coverage (defined by at least one BS within reach of the UE and outside the self-blockage zone) for open park scenario. The conditional probability and duration of dynamic blockage events are shown against BS density  $\lambda_T$  for various blocker densities  $\lambda_B$  and self-blockage angles  $\omega$ .

Table III: Simulation parameters

Parameters	Values
LOS Radius $\tilde{R}$	100 m
NLOS Radius $\tilde{R}$	65 m
Velocity of dynamic blockers $V$	1 m/s
Height of dynamic blockers $h_B$	1.8 m
Height of UE $h_R$	1.4 m
Height of BSs $h_T$	5 m
Expected blockage duration $1/\mu$	1/2 s
Self-blockage angle $\omega$	$60^\circ$
Parameter for number of NLOS Paths $\kappa$	3
Average size of static blockages $\ell \times w$	10 m $\times$ 10 m

### A. Open Park Scenario

For open areas, we conducted our analysis using both the stochastic geometry model and the hexagonal cell deployment. We consider two values of dynamic blocker density, 0.01 and 0.1 bl/m<sup>2</sup>, and two values of the self-blocking angle  $\omega$  (0 and 60°) for our study. We compare our analytical results using stochastic geometry with a MATLAB simulation<sup>2</sup>, where the movement of blockers is generated using the random waypoint mobility model [34], [35]. For the simulation, we consider a square box of size 200 m  $\times$  200 m with blockers located uniformly in this area. Our area of interest is the disc  $B(o, R)$  of radius  $R = 100$  m, which perfectly fits in the considered square area. The blockers choose a direction randomly and move in that direction for a time-duration of  $t \sim \text{Unif}[0, 60]$  sec. To maintain a fixed density of blockers in the square region, we consider that once a blocker reaches the edge of the square, it gets reflected. Note that for the given height of BSs, blockers, and the UE in Table III, we obtain from equation (7) that the blockers can block the LOS link only when they are within a range corresponding to a small fraction (11%) of the link length from the UE.

Figures 4(a), 4(b), and 4(c) present the statistics of LOS link blockages in the open park scenario. For the analysis of reliability, we obtained the blockage probability and expected blockage duration when the UE has at least one serving BS, i.e., the UE is always in the coverage area of at least one BS. From Figure 4(a), we can observe that the blockage probability decreases exponentially with BS density. For URLLC

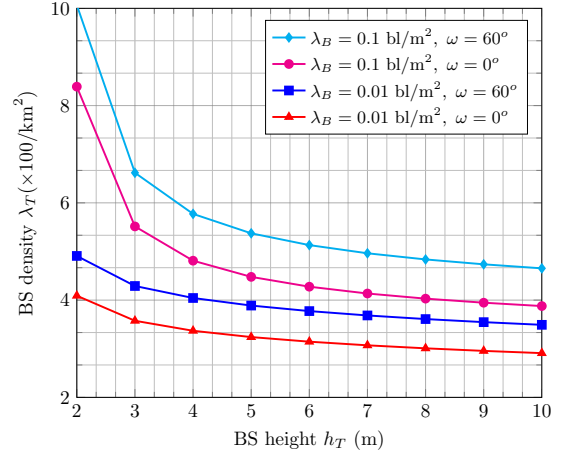


Figure 5: The trade-off between BS height and density for fixed dynamic blockage probability  $P(B^d|C^d) = 10^{-5}$ , for open park scenario.

applications, this means that only a dense mmWave cellular network can achieve high reliability. We may require around 400 BS/km<sup>2</sup> to achieve a blockage probability of  $10^{-5}$  or 99.999% service reliability for a blocker density of 0.01 bl/m<sup>2</sup> and self-blockage angle 60°. For a blocker density of 0.1 bl/m<sup>2</sup>, the required BS density is more than 400 BS/km<sup>2</sup>.

From Figure 4(c), we can observe that caching of 100 ms worth of data is required for a BS density 200/km<sup>2</sup> to have uninterrupted services. A BS density of 300/km<sup>2</sup> and 400/km<sup>2</sup> can bring down the required cached data to 60 ms and 50 ms, respectively. Furthermore, from Figure 4(b) and 4(c), we can observe that the interruption of 60 ms at a BS density of 300/km<sup>2</sup> occurs once in 1000 seconds for blocker density 0.01 bl/m<sup>2</sup>, and  $\omega = 60^\circ$ . This occasional high blockage duration (60 ms) may be acceptable for AR/VR applications. Thus, the cellular architecture needs to consider the optimal amount of cached data and the optimal BS density required to reduce the frequency of these high blockage durations to satisfy QoS requirements for AR/VR and other URLLC applications.

From Figure 4(a) and 4(b), we observe that both simulation and analytical results are approximately the same for a low blocker density of 0.01 bl/m<sup>2</sup>, but deviates modestly for high

<sup>2</sup>Our simulator MATLAB code is available at [github.com/ishjain/mmWave](https://github.com/ishjain/mmWave).

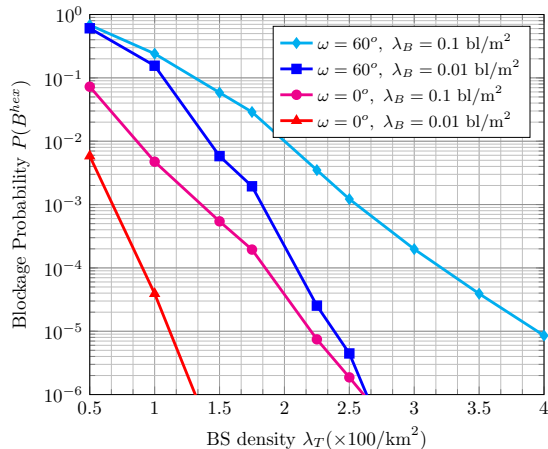


Figure 6: Blockage probability for hexagonal cells model for open park scenario.

BS densities when the blocker density is  $0.1 \text{ bl/m}^2$ . From Figure 4(c), we observe our analytical results follow closely the simulation results for low blocker density ( $0.01 \text{ bl/m}^2$ ). For a higher blocker density ( $0.1 \text{ bl/m}^2$ ) and low BS densities, the percentage deviation is large but still acceptable.

To increase the service reliability, apart from increasing the BS density, placing the BSs at a greater height may reduce the probability of blockage. The BS height vs. density trade-off is shown in Figure 5. Note, for example, that doubling the height of the BS from 4 m to 8 m reduces the BS density requirement by approximately 20%. The optimal BS height and density can be obtained by performing a cost analysis based on this trade-off.

Finally, we present the results for the hexagonal cell model in Figure 6 and compare them with that of the random model in Figure 4(a). Note that for deterministic locations of BSs in hexagonal cells case, we were unable to get the closed-form solution and we used numerical integration to evaluate the performance. For the self-blockage angle  $0^\circ$ , we observe that the blockage probability of  $10^{-5}$  can be achieved with about a half BSs (less than  $200 \text{ BS/km}^2$  for blocker density  $0.01 \text{ bl/m}^2$ , and less than  $300 \text{ BS/km}^2$  for blocker density  $0.1 \text{ bl/m}^2$ ). Next, we consider the self-blockage angle  $60^\circ$ , where we computed an upper bound on the blockage probability. In the hexagonal cell case, with a blocker density of  $0.01 \text{ bl/m}^2$  and self-blockage angle  $60^\circ$ , an upper bound of  $250 \text{ BS/km}^2$  will be sufficient to achieve  $10^{-5}$  blockage probability, which is quite low compared to that needed for the random topology in Figure 4(a) ( $400 \text{ BS/km}^2$ ).

### B. Urban Scenario

In an urban environment, the LOS paths to the UE may be blocked by buildings or permanent structures in addition to the dynamic and self-blockage. However, reflections from the buildings and other permanent structures may help in achieving higher coverage and service reliability by providing additional NLOS paths.

From Figure 7, we can observe that the coverage may degrade significantly due to static and self-blockage if the NLOS paths are not available. To achieve coverage of 90%

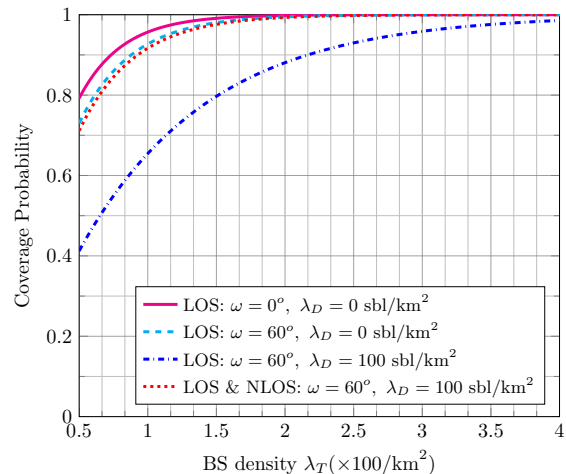
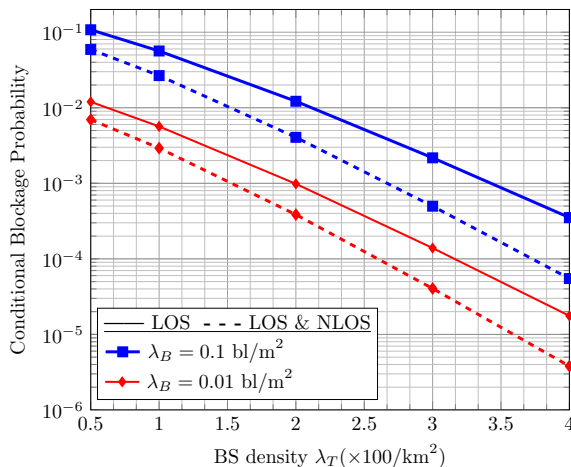


Figure 7: Coverage probability for both open park scenario and urban scenario.

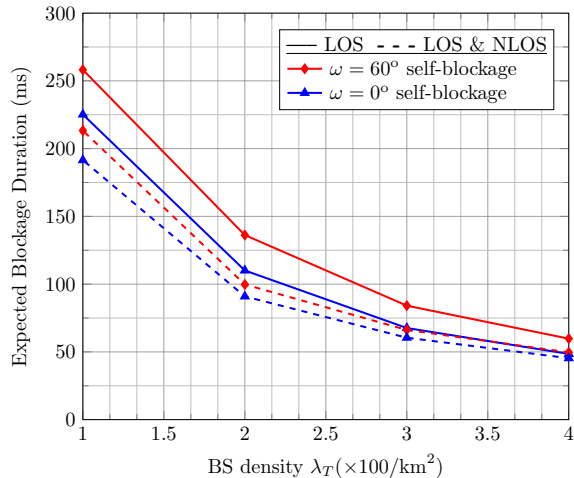
in the urban scenario, around  $200 \text{ BS/km}^2$  may be required in the absence of NLOS paths. However, to achieve 90% coverage in the presence of NLOS paths, significantly fewer BSs will be required ( $\sim 100 \text{ BS/km}^2$ ). Furthermore, prior work on a capacity analysis in [9] and [10] suggests that an even lower density of  $30\text{-}100 \text{ BS/km}^2$  should be enough to meet the capacity requirements of mmWave users.

Figure 8(a) and 8(b) present the blockage probability and duration in the urban scenario. It can be observed from Figures 7 and 8(a) that the design of mmWave cellular network may be limited by performance metrics such as blockage probability and the expected blockage duration instead of coverage or capacity. For instance, from Figure 8(a), we can observe that the blockage probability of  $10^{-5}$  requires a BS density higher than  $400 \text{ BS/km}^2$  in the urban scenario in the absence of strong NLOS paths. Similar observations can be concluded from Figure 8(b).

For NLOS links, we used the NLOS communication range of  $\tilde{R} = R \times 10^{-\frac{\gamma^{NLOS}}{10 \times \text{PLE}}}$ , where PLE is the path loss exponent and  $\gamma^{NLOS}$  is the attenuation (in dB) due to reflection of the signal. We use  $\text{PLE} = 2.69$  given by the path loss model in [9] at  $73 \text{ GHz}$  and assume an average attenuation of  $\gamma^{NLOS} = 5 \text{ dB}$ . We thus get the NLOS radius  $\tilde{R} = 65 \text{ m}$  corresponding to the LOS radius  $R = 100 \text{ m}$ . When NLOS paths are available, a high coverage probability can be achieved (See Figure 7) as compared to when NLOS paths are unavailable. Furthermore, from Figure 8(a) and 8(b), we can observe that NLOS paths provide a surprisingly modest benefit in achieving low probability of blockage and the expected blockage duration. However, the probability of blockage in the NLOS case is bounded by the fact that there is a high probability of not having any real BS within  $\tilde{R} = 65 \text{ m}$ , i.e., there is a high probability that the UE will not have any strong NLOS path. Thus, even with a rich scattered environment, NLOS paths cannot significantly help in achieving the required high reliability and low latency for URLLC applications. On the other hand, we can achieve significantly lower blockage probability if we assume high communication ranges for UE



(a) Conditional blockage Probability (given coverage).



(b) Expected blockage duration (given coverage).

Figure 8: Conditional blockage statistics given coverage (at least one BS not blocked by static or self-blockage) in the urban scenario considering 1) only LOS path, 2) both LOS and strong reflections (NLOS paths). We consider a static blockage density  $\lambda_D = 100$  sbl/km<sup>2</sup> and self-blockage angle  $\omega = 60^\circ$ . Note that blockage duration is independent of dynamic blocker density.

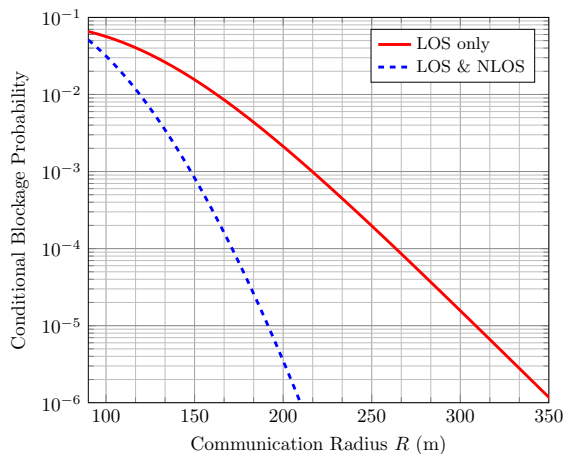


Figure 9: Conditional blockage probability (given coverage) in urban scenario vs communication radius of the UE with and without strong reflections. We chose BS density  $\lambda_T = 100$  BS/m<sup>2</sup>, self-blockage angle  $\omega = 60^\circ$ , dynamic blocker density  $\lambda_B = 0.1$  bl/m<sup>2</sup>, and static blockage density  $\lambda_D = 100$  sbl/m<sup>2</sup>.

as shown in Figure 9. Note that  $\tilde{R}$  scales linearly with  $R$ . Thus, with a higher communication radius  $R$  (and thus higher  $\tilde{R}$ ), we can achieve a significant reduction in blockage probability as compared to the LOS case. For instance, for the BS density of 100 BS/km<sup>2</sup>, the blockage probability of  $10^{-5}$  can be achieved at the range of  $R = 190$  m considering NLOS reflections, as compared to  $R = 310$  m using LOS paths alone. Recent improvements in mmWave transceiver technology may help achieve these higher ranges.

## VIII. CONCLUSIONS

In this paper, we presented simplified models to quantify key QoS parameters such as blockage probability and duration in mmWave cellular systems. We presented a generalized blockage analysis considering dynamic blockage due to mobile

blockers, static blockages due to buildings and permanent structures and self-blockage due to the user's own body. The user is considered blocked when LOS and NLOS paths to BS around the UE are blocked simultaneously. We verified our theoretical model with MATLAB simulations for self-blockage and dynamic blockages. For the scenarios we considered, our results indicate that the density of BS required to provide an acceptable quality of experience for URLLC applications is much higher than that obtained by capacity or coverage requirements. These results suggest that the mmWave cellular network engineering may be driven by dynamic blockage rather than capacity or coverage requirements. Furthermore, the blockage events may be correlated for multiple BSs based on the blocker's size and location. This correlation, which we did not model, may result in an even higher blockage probability. We also present an analysis of blockage probability for regularly spaced hexagonal cells and showed that such a planned mmWave cellular architecture could reduce blockages events as compared to more randomly allocated BS locations. As pointed out in the introduction, sub-6 GHz bands could be used to maintain connectivity during dynamic blockages, but this requires tight control plane integration between the mmWave and sub-6 GHz bands and careful traffic engineering to prevent the random traffic overflow from mmWave bands from overwhelming sub-6 GHz capacity. In the future, we plan to address this issue and issues related to correlation in blockage events.

## REFERENCES

- [1] W. Mohr, "5G empowering vertical industries," *Tech. Rep.*, 2016.
- [2] M. Bennis, M. Debbah, and H. V. Poor, "Ultra-reliable and low-latency wireless communication: Tail, risk and scale," *CoRR*, vol. abs/1801.01270, 2018. [Online]. Available: <http://arxiv.org/abs/1801.01270>
- [3] A. Seam *et al.*, "Enabling mobile augmented and virtual reality with 5G networks," *Tech. Rep.*, Jan 2017.
- [4] E. Baştuğ *et al.*, "Big data meets telcos: A proactive caching perspective," *Journal of Communications and Networks*, vol. 17, no. 6, pp. 549–557, Dec 2015.

- [5] E. Bastug, M. Bennis, and M. Debbah, "Living on the edge: The role of proactive caching in 5G wireless networks," *IEEE Communications Magazine*, vol. 52, no. 8, pp. 82–89, Aug 2014.
- [6] C.-P. Li *et al.*, "5G ultra-reliable and low-latency systems design," in *Proc. of IEEE EuCNC*, June 2017.
- [7] R. Kumar *et al.*, "Dynamic control of RLC buffer size for latency minimization in mobile RAN," in *Proc. of IEEE WCNC*, Apr. 2018.
- [8] T. S. Rappaport *et al.*, "Millimeter wave mobile communications for 5G cellular: It will work!" *IEEE Access*, vol. 1, pp. 335–349, May 2013.
- [9] M. R. Akdeniz *et al.*, "Millimeter wave channel modeling and cellular capacity evaluation," *IEEE J. Sel. Areas Commun.*, vol. 32, no. 6, pp. 1164–1179, June 2014.
- [10] T. Bai and R. W. Heath, "Coverage and rate analysis for millimeter-wave cellular networks," *IEEE Trans. Wireless Commun.*, vol. 14, no. 2, pp. 1100–1114, 2015.
- [11] G. R. MacCartney, T. S. Rappaport, and S. Rangan, "Rapid fading due to human blockage in pedestrian crowds at 5G millimeter-wave frequencies," in *Proc. of IEEE GLOBECOM*, Dec 2017.
- [12] G.-Y. P. Kim, J. A. C. Lee, and S. Hong, "Analysis of macro-diversity in LTE-advanced," *KSII Transactions on Internet and Information Systems*, vol. 5, no. 9, pp. 1596–1612, 2011.
- [13] Y. Lin *et al.*, "Wireless network cloud: Architecture and system requirements," *IBM Journal of Research and Development*, vol. 54, no. 1, pp. 4:1–4:12, Jan. 2010.
- [14] K. Chen and R. Duan, "C-RAN the road towards green RAN," *China Mobile Research Institute, white paper*, vol. 2, 2011.
- [15] A. Checko *et al.*, "Cloud RAN for mobile networks – a technology overview," *IEEE Communications Surveys Tutorials*, vol. 17, no. 1, pp. 405–426, Firstquarter 2015.
- [16] "4G-5G interworking RAN-level and CN-level interworking," Tech. Rep., June 2017. [Online]. Available: <https://bit.ly/2tiTRY>
- [17] E. Bastug *et al.*, "Toward interconnected virtual reality: Opportunities, challenges, and enablers," *IEEE Commun. Mag.*, vol. 55, no. 6, pp. 110–117, 2017.
- [18] C. Westphal, "Challenges in networking to support augmented reality and virtual reality," in *Proc. of IEEE ICNC*, 2017.
- [19] T. Bai, R. Vaze, and R. W. Heath, "Using random shape theory to model blockage in random cellular networks," in *Proc. of IEEE SPCOM*, Aug. 2012.
- [20] T. Bai and R. W. Heath, "Analysis of self-body blocking effects in millimeter wave cellular networks," in *Proc. of IEEE Asilomar*, Nov. 2014.
- [21] "Study on channel model for frequencies from 0.5 to 100 GHz (release 14)," 3GPP TR 38.901 V14.1.1, Jul. 2017.
- [22] M. Gapeyenko *et al.*, "Analysis of human-body blockage in urban millimeter-wave cellular communications," in *Proc. of IEEE ICC*, July 2016.
- [23] Y. Wang *et al.*, "Blockage and coverage analysis with mmwave cross street BSs near urban intersections," in *Proc. of IEEE ICC*, July 2017.
- [24] V. Raghavan *et al.*, "Statistical blockage modeling and robustness of beamforming in millimeter wave systems," *arXiv preprint arXiv:1801.03346*, 2018.
- [25] B. Han, L. Wang, and H. D. Schotten, "A 3D human body blockage model for outdoor millimeter-wave cellular communication," *Physical Communication*, vol. 25, pp. 502–510, 2017.
- [26] A. Samuylov *et al.*, "Characterizing spatial correlation of blockage statistics in urban mmWave systems," in *Proc. of IEEE Globecom Workshops*, Dec. 2016.
- [27] M. Gapeyenko *et al.*, "On the temporal effects of mobile blockers in urban millimeter-wave cellular scenarios," *IEEE Trans. Veh. Technol.*, vol. 66, no. 11, pp. 10 124–10 138, Nov 2017.
- [28] M. Abouelseoud and G. Charlton, "The effect of human blockage on the performance of millimeter-wave access link for outdoor coverage," in *Proc. of IEEE VTC Spring*, June 2013.
- [29] Y. Zhu *et al.*, "Leveraging multi-AP diversity for transmission resilience in wireless networks: architecture and performance analysis," *IEEE Trans. Wireless Commun.*, vol. 8, no. 10, pp. 5030–5040, Oct. 2009.
- [30] X. Zhang *et al.*, "Improving network throughput in 60GHz WLANs via multi-AP diversity," in *Proc. of IEEE ICC*, June 2012.
- [31] J. Choi, "On the macro diversity with multiple BSs to mitigate blockage in millimeter-wave communications," *EEE Commun. Lett.*, vol. 18, no. 9, pp. 1653–1656, 2014.
- [32] A. K. Gupta, J. G. Andrews, and R. W. Heath, "Macrodiversity in cellular networks with random blockages," *IEEE Trans. Wireless Commun.*, vol. 17, no. 2, pp. 996–1010, 2018.
- [33] I. K. Jain, R. Kumar, and S. Panwar, "Driven by capacity or blockage? a millimeter wave blockage analysis," to appear in *Proc. of 30th International Teletraffic Congress (ITC 30)*, Sep. 2018.
- [34] D. B. Johnson and D. A. Maltz, *Dynamic Source Routing in Ad Hoc Wireless Networks*. Boston, MA: Springer US, 1996, pp. 153–181.
- [35] M. Boutin, "Random waypoint mobility model," <https://www.mathworks.com>, accessed: 2018-03-18.

## APPENDIX

### A. Proof of Lemma 2

The probability that a BS-UE link is not blocked (by static or self-blockage) follows from the independence of static blockage and self-blockage. Utilizing the expressions of static and self-blockage from (3) and (4) respectively, and taking average over the distance distribution  $f_{R_i|M}(r|m)$  from (2), we get,

$$\begin{aligned} P(\text{a BS is in coverage}|m) &= \int_{r=0}^R pe^{-(\beta r + \beta_0)} \frac{2r}{R^2} dr \\ &= pq, \end{aligned} \quad (48)$$

where  $q = \int_{r=0}^R e^{-(\beta r + \beta_0)} \frac{2r}{R^2} dr$  is solved to a closed-form expression given in (13). We assume that all the  $m$  BSs in the disc  $B(o, R)$ , each BS may get blocked independently with probability  $pq$ . Therefore, the distribution of the number of BSs  $N$  which are not blocked by static or self-blockage follows a geometric distribution,

$$P_{N|M}(n|m) = \binom{m}{n} (pq)^n (1 - pq)^{m-n}. \quad (49)$$

Taking the average over the distribution  $P_M(m)$  given in (1), we get the distribution of  $N$  as follows:

$$\begin{aligned} P_N(n) &= \sum_{m=0}^{\infty} P_{N|M}(n|m) P_M(m) \\ &= \sum_{m=0}^{\infty} \binom{m}{n} (pq)^n (1 - pq)^{m-n} \frac{[\lambda_T \pi R^2]^m}{m!} e^{-\lambda_T \pi R^2} \\ &= \frac{[pq \lambda_T \pi R^2]^n}{n!} e^{-pq \lambda_T \pi R^2}. \end{aligned} \quad (50)$$

This concludes the proof of Lemma 2.

### B. Proof of Theorem 1

The probability  $P(B^{LOS}|m)$  in (17) is given by

$$\begin{aligned}
P(B^{LOS}|m) &= \iint_{r_i} P(B^{LOS}|m, \{r_i\}) f(\{r_i\}|m) dr_1 \cdots dr_m, \\
&= \iint_{r_i} \prod_{i=1}^m \left( 1 - pe^{-(\beta r_i + \beta_0)} \frac{1}{1 + \frac{C}{\mu} r_i} \right) \\
&\quad \times f(r_i|m) dr_1 \cdots dr_m, \\
&= \prod_{i=1}^m \int_{r=0}^R \left( 1 - pe^{-(\beta r + \beta_0)} \frac{1}{1 + \frac{C}{\mu} r} \right) \frac{2r}{R^2} dr \\
&= \left( \int_{r=0}^R \left( 1 - pe^{-(\beta r + \beta_0)} \frac{1}{1 + \frac{C}{\mu} r} \right) \frac{2r}{R^2} dr \right)^m \\
&= \left( 1 - p \int_{r=0}^R \frac{e^{-(\beta r + \beta_0)} 2r}{1 + \frac{C}{\mu} r} \frac{dr}{R^2} \right)^m \\
&= (1 - ap)^m
\end{aligned} \tag{51}$$

where we defined  $a$  in (21). We now evaluate  $P(B^{LOS})$  in (18) as

$$\begin{aligned}
P(B^{LOS}) &= \sum_{n=0}^{\infty} P(B^{LOS}|m) P_M(m) \\
&= \sum_{m=0}^{\infty} (1 - ap)^m \frac{[\lambda_T \pi R^2]^m}{m!} e^{-\lambda_T \pi R^2} \\
&= e^{-ap \lambda_T \pi R^2}.
\end{aligned} \tag{52}$$

Finally, the conditional blockage probability  $P(B^{LOS}|\mathcal{C}^{LOS})$ , conditioned on the coverage event  $\mathcal{C}^{LOS}$ , is obtained as follows:

$$P(B^{LOS}) = P(B^{LOS}|\mathcal{C}^{LOS})P(\mathcal{C}^{LOS}) + 1 - P(\mathcal{C}^{LOS}) \tag{53}$$

and therefore,

$$\begin{aligned}
P(B^{LOS}|\mathcal{C}^{LOS}) &= \frac{P(B^{LOS}) - (1 - P(\mathcal{C}^{LOS}))}{P(\mathcal{C}^{LOS})} \\
&= \frac{e^{-ap \lambda_T \pi R^2} - e^{-pq \lambda_T \pi R^2}}{1 - e^{-pq \lambda_T \pi R^2}}.
\end{aligned} \tag{54}$$

This concludes the proof of Theorem 1.

We follow with the proof of Corollary 2. We first derive  $P(B^d|m)$  similar to (51), but by setting  $\beta = \beta_0 = 0$  for the dynamic blockage case. Therefore, the expression of  $a$  in (21) gets simplified and is represented by  $a'$  as follows:

$$\begin{aligned}
a' &= \int_{r=0}^R \frac{1}{1 + \frac{C}{\mu} r} \frac{2r}{R^2} dr \\
&= \frac{2\mu}{RC} - \frac{2\mu^2}{R^2 C^2} \log \left( 1 + \frac{RC}{\mu} \right),
\end{aligned} \tag{55}$$

where the intermediate steps of integration are omitted for brevity. The rest of the analysis is similar to the derivation in (52) and (54).

### C. Proof of Theorem 2

Using the results from (28), we find the expected blockage duration  $\mathbb{E}[T^{LOS}|\mathcal{C}^{LOS}]$ , conditioned on the coverage event  $\mathcal{C}^{LOS}$  defined in (14), as follows:

$$\begin{aligned}
\mathbb{E}[T^{LOS}|\mathcal{C}^{LOS}] &= \frac{\sum_{n=1}^{\infty} \frac{1}{n\mu} P_N(n)}{P(\mathcal{C}^{LOS})} \\
&= \frac{\sum_{n=1}^{\infty} \frac{1}{n\mu} \frac{[pq \lambda_T \pi R^2]^n}{n!} e^{-pq \lambda_T \pi R^2}}{1 - e^{-pq \lambda_T \pi R^2}} \\
&= \frac{e^{-pq \lambda_T \pi R^2}}{\mu (1 - e^{-pq \lambda_T \pi R^2})} \sum_{n=1}^{\infty} \frac{[pq \lambda_T \pi R^2]^n}{nn!}.
\end{aligned} \tag{56}$$

This concludes the proof of Theorem 2.

### D. Proof of approximation of Expected Duration

The expectation of a function  $f(n) = 1/n$  can be approximated using the Taylor series as

$$\begin{aligned}
\mathbb{E}[f(n)] &= \mathbb{E}(f(\mu_n + (x - \mu_n))), \\
&= \mathbb{E}[f(\mu_n) + f'(\mu_n)(x - \mu_n) + \frac{1}{2}f''(\mu_n)(x - \mu_n)^2] \\
&\approx f(\mu_n) + \frac{1}{2}f''(\mu_n)\sigma_n^2 \\
&= \frac{1}{\mu_n} + \frac{\sigma_n^2}{\mu_n^3},
\end{aligned} \tag{57}$$

where  $\mu_n$  and  $\sigma_n^2$  are the mean and variance of Poisson random variable  $N$  given in (12). We get the required expression by substituting  $\mu_n = pq \lambda_T \pi R^2$  and  $\sigma_n^2 = pq \lambda_T \pi R^2$  as follows:

$$\mathbb{E}[1/n] \approx \frac{1}{pq \lambda_T \pi R^2} + \frac{1}{(pq \lambda_T \pi R^2)^2}. \tag{58}$$

On further simplification for high BS densities, we can further approximate the expression as:

$$\mathbb{E}[1/n] \approx \frac{1}{pq \lambda_T \pi R^2} = \frac{1}{\mathbb{E}[n]}. \tag{59}$$

Using (59), we approximate  $\mathbb{E}[T^{LOS}|\mathcal{C}^{LOS}]$  as follows:

$$\begin{aligned}
[T^{LOS}|\mathcal{C}^{LOS}] &\approx \frac{1}{P(n \neq 0)\mu \mathbb{E}[n, n \neq 0]} \\
&= \frac{1}{P(\mathcal{C}^{LOS})\mu pq \lambda_T \pi R^2}.
\end{aligned} \tag{60}$$

Finally, the expression in (30) can be obtained by substituting  $P(\mathcal{C}^{LOS})$  from (14) to (60).

### E. Proof of Theorem 3

Note that the probability  $P(B_i^d|n, \{r_i\})$  follows the same expression as  $P(B_i^d|m, \{r_i\})$  in (11) in the absence of static blockages. Therefore, we simplify  $\zeta^d$  in (32) as follows:

$$\zeta^d = n\mu \prod_{i=1}^n \frac{\frac{C}{\mu} r_i}{1 + \frac{C}{\mu} r_i}. \tag{61}$$

We first evaluate  $\mathbb{E}[\zeta^d|n]$  as follows:

$$\begin{aligned}\mathbb{E}[\zeta^d|n] &= n\mu \left( \int_r \frac{\frac{C}{\mu} r}{1 + \frac{C}{\mu} r} \frac{2r}{R^2} dr \right)^n \\ &= n\mu(1 - a')^n,\end{aligned}\quad (62)$$

where the intermediate steps are similar to the derivation of (55). Next, we evaluate  $\mathbb{E}[\zeta^d]$  as follows:

$$\begin{aligned}\mathbb{E}[\zeta^d] &= \sum_{n=0}^{\infty} n\mu(1 - a')^n \frac{[p\lambda_T\pi R^2]^n}{n!} e^{-p\lambda_T\pi R^2} \\ &= \mu(1 - a')p\lambda_T\pi R^2 e^{-ap\lambda_T\pi R^2} \times \\ &\quad \sum_{n=0}^{\infty} \frac{[(1 - a')p\lambda_T\pi R^2]^{(n-1)}}{(n-1)!} e^{-(1-a')p\lambda_T\pi R^2} \\ &= \mu(1 - a')p\lambda_T\pi R^2 e^{-a'p\lambda_T\pi R^2}.\end{aligned}\quad (63)$$

Finally, the expected frequency of blockage conditioned on the coverage  $C^d$  (22) is given by

$$\begin{aligned}\mathbb{E}[\zeta^d|C^d] &= \frac{\sum_{n=1}^{\infty} \mathbb{E}[\zeta^d|n]P_N(n)}{P(C^d)} = \frac{\sum_{n=0}^{\infty} \mathbb{E}[\zeta^d|n]P_N(n)}{P(C^d)} \\ &= \frac{\mu(1 - a')p\lambda_T\pi R^2 e^{-a'p\lambda_T\pi R^2}}{1 - e^{-p\lambda_T\pi R^2}}.\end{aligned}\quad (64)$$

This concludes the proof of Theorem 3.

#### F. Proof of Lemma 4

Assuming the independence of LOS and NLOS links, we obtain the coverage probability  $P(C)$  as follows:

$$\begin{aligned}P(C) &= \sum_m \iint_{r_i} P(C|m, r_i) f(\{r_i\}|m) d\{r_i\} P_M(m) \\ &= \sum_m \iint_{r_i} \left( 1 - \prod_{i=1}^m (1 - pe^{-(\beta r_i + \beta_0)}) I_{(r_i > \bar{R})} \right) \\ &\quad \times f(\{r_i\}|m) d\{r_i\} P_M(m) \\ &= 1 - \sum_m \left( \int_{r=\bar{R}}^R (1 - pe^{-(\beta r + \beta_0)}) \frac{2r}{R^2} dr \right)^m P_M(m).\end{aligned}\quad (65)$$

We define

$$\tilde{q} = 1 - \int_{r=\bar{R}}^R (1 - pe^{-(\beta r + \beta_0)}) \frac{2r}{R^2} dr, \quad (66)$$

and solve the integration in (66) to a closed-form expression given in (36). Finally, we evaluate the coverage probability (35) by following the steps similar to the derivation of (52).

#### G. Extending Blockage Model to Multiple BSs through Markov Chain Analysis

Since the blockage events form an alternating renewal process with exponentially distributed durations of blocked and unblocked intervals, we formulate a Markov chain to obtain the probability and duration of the simultaneous blockage of  $k$  BSs, out of the total  $n$  available BSs<sup>3</sup>.

<sup>3</sup>Note that we reuse the variable  $k$  here, since the meaning is clear from the context.

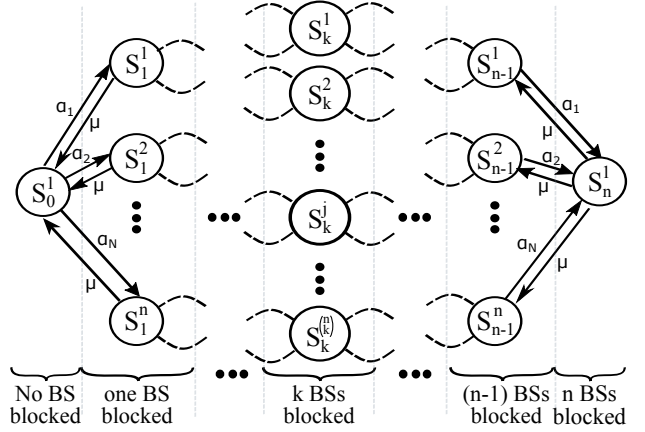


Figure 10: Markov Chain for  $N$  BSs

The Markov chain shown in Figure 10 has  $2^n$  states where each state represents the blockage of a subset of  $n$  BSs. Let a set  $S = \{1, 2, \dots, n\}$  represents the  $n$  BSs. Define  $\mathcal{P}(S)$  as a power set of  $S$  of size  $2^n$ . The elements of  $\mathcal{P}$  can be represented by a set  $S_k^j$  for  $j = 1, \dots, \binom{n}{k}$  and  $k = 0, \dots, n$ . Note that the set  $S_k^j$  is associated with the state  $S_k^j$  of our Markov model shown in Figure 10. Also, it is clear that the total number of states are  $\sum_{k=0}^n \binom{n}{k} = 2^n$ . We are interested in the probability of the last state ( $S_n^1$ ), since it represents the probability that all  $n$  available BSs are blocked.

**Lemma 5.** Let  $P_n^1$  denote the probability of the last state ( $S_n^1$ ) of the Markov model in Figure 10, then

$$P_n^1 = \prod_{i=1}^n \frac{\alpha_i/\mu}{1 + \alpha_i/\mu} = \prod_{i=1}^n \frac{\frac{C}{\mu} r_i}{1 + \frac{C}{\mu} r_i}, \quad (67)$$

where  $C$  is defined in (9).

*Proof.* The equilibrium steady-state distribution exists when  $\alpha_i < \mu$ ,  $\forall i = 1 : n$ .

The steady-state probabilities of our Markov model in Figure 10 are computed as

$$P_k^j = \prod_{l \in S_k^j} \frac{\alpha_l}{\mu} P_0^1, \quad j = 1, \dots, \binom{n}{k}, \quad k = 1, \dots, n, \quad (68)$$

where  $P_0^1$  represents the probability of the state  $S_0^1$ . By putting the sum of all state probabilities to 1, We obtain

$$P_0^1 = \frac{1}{1 + \sum_{k=1}^n \sum_{j=1}^{\binom{n}{k}} \prod_{l \in S_k^j} \frac{\alpha_l}{\mu}} = \frac{1}{\prod_{i=1}^n (1 + \alpha_i/\mu)} \quad (69)$$

Therefore, the state probabilities become

$$P_k^j = \frac{\prod_{l \in S_k^j} \frac{\alpha_l}{\mu}}{\prod_{i=1}^n (1 + \alpha_i/\mu)}, \quad j = 1, \dots, \binom{n}{k}, \quad k = 1, \dots, n. \quad (70)$$

Note the sum of state probabilities for  $j = 1, \dots, \binom{n}{k}$  and for fixed  $k$  represents the probability  $P_k$  of the blockage of  $k$  BSs, i.e.,

$$P_k = \sum_{j=1}^{\binom{n}{k}} P_k^j = \frac{\sum_{j=1}^{\binom{n}{k}} \prod_{l \in S_k^j} \frac{\alpha_l}{\mu}}{\prod_{i=1}^n (1 + \alpha_i/\mu)}, \quad k = 1, \dots, n. \quad (71)$$

By putting  $k = n$ , we get the probability that all  $n$  BSs are blocked

$$P_n^1 = \frac{\sum_{j=1}^{\binom{n}{n}} \prod_{l=1}^n \frac{\alpha_l}{\mu}}{\prod_{i=1}^n (1 + \alpha_i/\mu)} = \prod_{i=1}^n \frac{\alpha_i/\mu}{1 + \alpha_i/\mu}. \quad (72)$$

■